Taylor & Francis
Taylor & Francis Group

SEPARATION SCIENCE AND TECHNOLOGY

Separation Science and Technology

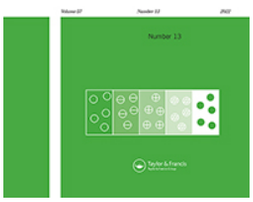

ISSN: (Print) (Online) Journal homepage: www.tandfonline.com/journals/lsst20

Extracting salt from hypersaline water by pulsed corona discharge

Kristy Emanuel Silva Fontes, Liliane Ferreira Araújo de Almada, Jussier de Oliveira Vitoriano & Clodomiro Alves Júnior

To cite this article: Kristy Emanuel Silva Fontes, Liliane Ferreira Araújo de Almada, Jussier de Oliveira Vitoriano & Clodomiro Alves Júnior (2022) Extracting salt from hypersaline water by pulsed corona discharge, Separation Science and Technology, 57:13, 2065-2072, DOI: 10.1080/01496395.2021.2017969

To link to this article: https://doi.org/10.1080/01496395.2021.2017969

Published online: 27 Dec 2021.

SEPARATION SCIENCE AND TECHNOLOGY
2022, VOL. 57, NO. 13, 2065–2072
https://doi.org/10.1080/01496395.2021.2017969

Taylor & Francis
Taylor & Francis Group

Extracting salt from hypersaline water by pulsed corona discharge

Kristy Emanuel Silva Fontes[a], Liliane Ferreira Araújo de Almada[a], Jussier de Oliveira Vitoriano[b], and Clodomiro Alves Júnior[a,b]

[a]Department of Department of Natural Sciences, Mathematics and Statistics, Federal Rural University of Semiarid, Mossoró, Brazil; [b]Department of Mechanical Engineering, Federal University of Rio Grande Do Norte, Campus Universitário S/n, Natal, Brazil

ABSTRACT

Seawater bittern is obtained as a by-product of the solar salt industry or saline water conversion plants. This product is rich in Mg^{2+}, Cl^{-}, SO_4^{2-}, K^{+}, as well as Na^{+} ions. In the present work, we investigated the chemical products of seawater extraction during the conventional evaporation-crystallization process, when plasma is applied over the solution. In the present work, we investigated the chemical products of seawater extraction during the conventional evaporation-crystallization process, when plasma is applied over the solution. Crystal films were formed on the surface, both in the region surrounding the plasma application and far regions. However, the films in the vicinity of the discharge had grain sizes up to 97% smaller than those of natural evaporation. We also observed that the region close to the plasma produces salt with higher Mg/Na and K/Na ratios than in the sedimented salts, indicating greater selectivity of the plasma process. This study adds to the growing body of research that indicates plasma as energy source in the desalination or separation processes.

ARTICLE HISTORY
Received 24 June 2021
Accepted 9 December 2021

KEYWORDS
Extraction; plasma; desalination; activated crystallization; selectivity

Introduction

Saline effluents from salt production in the solar salt industry or desalination plants, have high concentration of different ions such as Mg^{2+}, Cl^{-}, SO_4^{2-}, K^{+}, Cl^{-} and Na^{+}. In these ionic concentrations the salts are precipitated simultaneously and then make it difficult to extract relatively pure salts by evaporation, so it is usually treated as waste.[1] A considerable amount of literature has been published aiming separate this solution here called hypersaline water. Based on liquid-liquid extraction (LLE) processes,[2,3] including directional solvent extraction desalination (DSE)[4,5] and liquid phase microextraction (LPME), overcome the main disadvantages of LLE, such as a relatively long time of analysis (especially when evaporation and reconstitution are required), high consumption of solvents, and its tedious application.[6] However, any liquid-liquid extraction technique generates organic waste which requires disposal and in some cases the need for solvent regeneration.[7] Techniques of particular interest are those which do not result in disposal such as salt separation preferential (SSP).[8] Among mineral extraction commercial from seawater without organic waste, the electrolytic processes are more economic.[9] There is a growing body of literature that recognizes that plasma over liquid solution lead to electrolytic reactions.[10] Analogous to conventional electrochemistry with solid metal electrodes; in the case of electrons flowing from plasma over surface solution, cathodic (i.e. reduction) reactions should occur and electrons may become solvated and initiate complex reactions at the surface or in the bulk of the solution and electrons could cause direct dissociation of molecules (e.g.water) via electron-impact dissociation.[11] We have recently shown that the application of pulsed corona discharge (PCD) on hypersaline solution induces crystal formation on the surface.[12,13] This phenomenon of precipitation on the water surface is also observed during the manufacture of sea salt, under specific climatic conditions, light winds, high temperature and low relative humidity.[14] In the salt pans, the crystals formed on the surface of these waters constitute the first collection of salt and are called flower of salt. Its crystals have white color, are less compact, have high fragility and high commercial value.[15] We observed that in PCD the size, morphology, and growth rate of the crystals are different from those produced in the natural evaporation process. It is not easy to separate the effect of electric field in the molecular structure and the localized ohmic heating produced by the electric

CONTACT Clodomiro Alves Júnior clodomiro.jr@ufersa.edu.br Rural Federal University of Semiarid, Av. Francisco Mota, 572 - Bairro Costa e Silva, Mossoró RN | CEP: 59.625-900, Brazil

current crossing the liquid, to explain the accelerated salt crystallization. We hypothesized that water dipole alignment caused by electric field might be able to cause crystallization once the external electric field competes with the field of individual ions. Thus, we have unidirectional dipole alignment versus central dipole alignment around ions. Due to this, the external field weakens the solvation of ions. Less solvated ions are more prone to form pairs, clusters and eventually precipitate. This study aims to contribute to this growing area of research by exploring the influence of PCD on selective salt precipitation. Since the bittern is composed of many ions with different electrical charges, a selective separation of these ions is expected by the action of the plasma electric field.

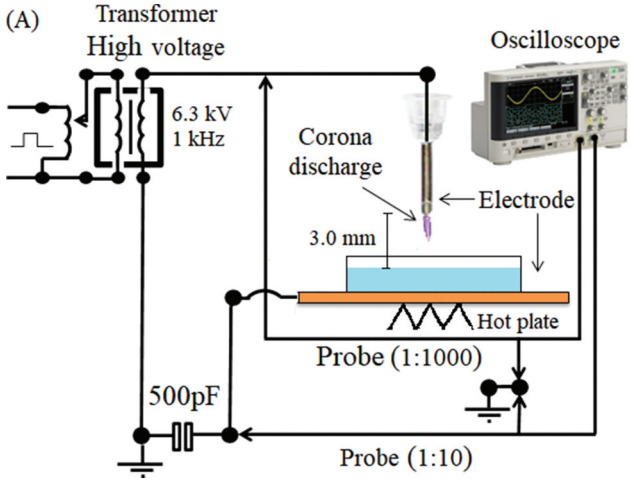

Figure 1. Experimental apparatus used in the plasma treatment of bittern, using a PCD configuration.

Materials and methods

Sample preparation

The bittern sample containing 450 gL^{-1} of solid and density 1.235 $g.cm^{-3}$ is extracted from a salt-work in Grossos/RN-Brazil. It was filtrated and then characterized in terms of density, electrical conductivity, and pH, in addition to chemical analysis (Table 1). The pH measurements were performed with the aid of a Bel bench pH meter (model PHS3BW with Kasvi glass electrode, model K38-1465, coupled); electrical conductivity, with the aid of a conductivity meter (Resistivity/TDS/NaCl Hanna, model HI98192); density using a pycnometer (25 ml).

The samples were chemically analyzed to determine the concentrations of Na^+, K^+, Ca^{2+}, Mg^{2+}, Cl^- and SO_4^{2-} ions. The ionic concentrations of sodium, calcium and potassium were determined with the aid of a Digimed flame photometer, model DM-62. The concentration of the sulfate ion was determined by optical absorption spectroscopy, using the turbidimetric method on a UV-VIS spectrophotometer, model Genesys 10S. The Cl^- and Mg^{2+} ions were determined by the Mohr method and by complexometric titration, respectively. Mg^{2+} concentrations were determined by the difference between the water hardness and the concentration of Ca^{2+} ions. The titrant for determining the hardness consisted of a 0.001 M and 0.1 M EDTA solution for salt samples and solution, respectively. All analyses were performed in triplicate.

Plasma treatments

Plasma treatment was performed using an experimental apparatus as depicted schematically in the Fig. 1. In a cylindrical polypropylene container (100 mm x 100 mm x 50 mm), 300 ml of bittern was placed, which was evaporated with the aid of a heating plate maintained at 40°C, to simulate the evaporation on salt-work. When the first crystals started to form on surface, a stainless-steel needle (1.20 mm x 40.0 mm) with a conical end (tip radius 0.27 mm), negatively polarized was positioned 3.0 mm above the bittern surface. A grounded copper plate (1.0 mm x 100.0 mm x 100.0 mm) was positioned below of the polypropylene recipient. In this moment, a pulsed voltage source set at 6.3 kV, repeated with a frequency of 1.0 kHz was triggered to generate the PCD over the bittern during 0.08 h. After 3 h of evaporation, the produced crystals and aliquots of the solution were extracted and characterized. This process was repeated 13 times, for every 3 hours of evaporation. Plasma diagnosis was performed with the aid of an optical emission spectrometer USB 4000 UV-VIS, Ocean Optics.

The process was carried out under a Nikon MSZ 18 stereoscopic magnifying glass attached to a Nikon DS-F12 camera with a frame rate of 20 fps. The ambient temperature and relative humidity were kept at 25°C and 50%, respectively. The dynamics of the crystallization promoted by the plasma on the bittern surface was filmed. The crystals formed on surface were evaluated in

Table 1. Characterization of raw material.

Density (g/cm^3)	pH	Electrical conductivity (mS/cm)	Ion concentration ($g.L^{-1}$)					
			Na^+	Mg^{2+}	Ca^+	K^+	Cl^-	$(SO_4)^{2-}$
1.235	7.0	172	71.5	19.8	2.7	8.1	170.6	27.3

situ for their morphology using a stereoscopic microscope. Image analysis was used to measure the area of the film and grain size. Each evaporation essay lasted 39 h, divided at interval of 3 h, when the salts samples and aliquot from bittern are extracted for characterization. As expected, due to the loss of water from the bittern through evaporation, the density increased from 1.235 g/cm^3 to 1.255 g/cm^3.

Samples characterization

At the end of each 3 h interval, both the salt film formed in the region close to the plasma application point and those formed on the surface of the other regions, were extracted for analysis. These materials had quite different characteristics. While the crystals formed in the distant region of the discharge showed transparency, with large and dispersed grains, the film around the discharge was dense, white in color and small grains. Samples taken from regions far from the discharge were called flower of salt (FS), due to the similarity with the flower of salt produced through the evaporation of supersaturated sea water, which is very popular in the cuisine of different countries in the world.[14,16] The film formed in the vicinity of the discharge was called dense flower of salt (DFS). In addition to these samples, salts sedimented at the bottom of the container (SED) were also collected after precipitation. These samples were placed in an oven at 60°C for drying until the weight remained constant, for further chemical analysis. For analysis of the solution, a 1 ml aliquot of the bittern was dried, and the weight recorded. For chemical analysis, 20 mg of the samples were diluted in 50 ml of deionized water, resulting in a concentration of 400 mg/L, as described in 2.1. For each result, an average of the value of three analyses, performed on three different samples, was performed. Microstructural analysis was performed with the aid of a stereoscopic magnifying glass (Nikon MSZ 18) and scanning electron microscope (SEM – Tescan Vega 3).

Results

Precipitation dynamics of flower of salt

During our experiments, the formation of the flower of salt was observed on the surface of the bittern with two different characteristics (Fig. 2). While the film formed in regions far from the discharge showed transparency, with large and dispersed grains (Fig. 2A and B), the film in the vicinity of the discharge was dense, intense white in color and small grains (Fig. 2A, C, D). The mechanism by which this film is formed on the surface is not yet well known, although it is known that temperature, wind speed and relative humidity are important variables in the process.[16,17] It was also observed that a saline bridge (SB) (Fig. 2A), between the DFS film and the stainless-steel needle (cathode) was formed. During the process, the presence of bubbles was observed, in a convection movement produced by the thermal gradient from the bottom to the surface. There is a correlation between the reduction of bubbles and the appearance of FS crystals. It is possible that the presence of these bubbles is essential for the formation of crystals on the surface, since they are preferred sites for the nucleation of salts,[18] in addition to increasing the buoyancy of the crystals. In the case of DFS crystals, which have a higher nucleation speed, confirmed by the smaller size of the grains (Fig. 2D), it is clear that the plasma also influences the precipitation mechanism. Plasma-assisted precipitation details were obtained recently by looking at a pulsed corona discharge over a droplet of bittern.[13] A deformation of the water surface like a cone was firstly observed from water surface to cathode was firstly observed and then crystals precipitation inside the cone. This effect has been demonstrated as a orientational reordering of the water molecules with their dipole moments parallel to the field, resulting in chains of aligned molecular dipole moments.[18]

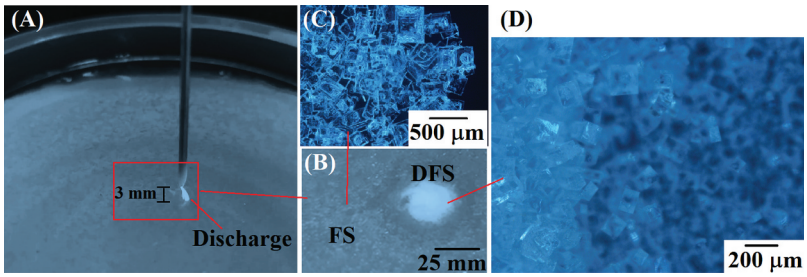

Figure 2. (A) Different regions observed during the application of plasma on the bittern surface. (B) Details of the salt flower precipitated at the plasma application point (DFS) and away from the discharge (FS); (C) Details of crystal structure of FS and (D) Details of the region in the vicinity of the discharge, showing amorphous crystal and micro crystals in the point where the discharge was applied.

Film structure and salt precipitation kinetics

In general, the DFS film has grains with sizes that increase radially from the point of application of the plasma to the periphery (Fig. 3). Another important finding was that in more concentrated solutions (solutions with higher density due longer evaporation time), the amount of DFS was lower, although in this range of density values the solution is supersaturated for NaCl, $MgCl_2$, $MgSO_4$ and KCl salts. In fact, there was precipitation, but this happened mainly in the volume of the solution, and the precipitates were sedimented afterward. This means that there was a reduction in the factors responsible for the mechanism of the nucleation of salts on the surface. Despite the scarce literature on the subject, it is known that surface temperature and humidity are important variables for the formation of the flower of salt. Since there was no variation in these quantities, a possible explanation for this might be attributed to the density of bubbles, which were visible during the process.[19]

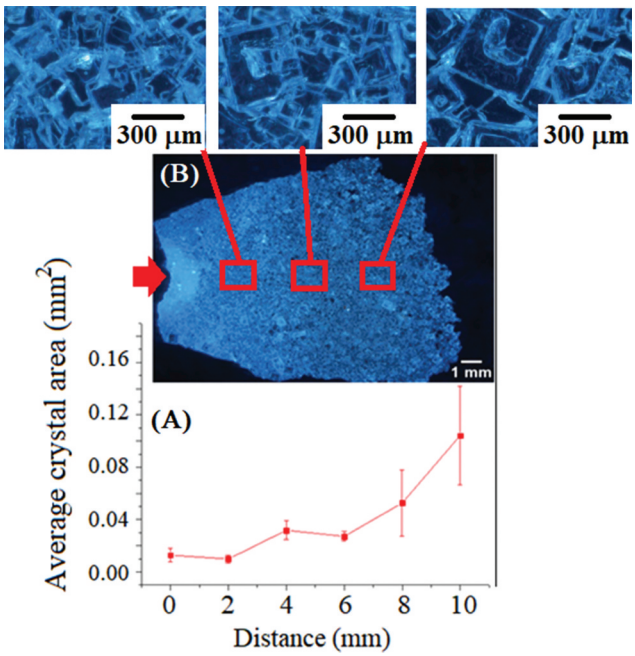

Figure 3. (A) Average area of the crystals for the different regions of the DFS grain shown (B), from the plasma application point (red arrow) to the film periphery. Details of the crystal structure are shown above.

Previous studies have already observed that the number of bubbles in salt water is an order of magnitude higher than in fresh water for bubbles with radii greater than 100 mm.[20] Although monitoring was not carried out during all the experiments, larger number and size of bubbles were observed for solutions with lower densities. The higher ion concentration can affect the floatability of the minerals as well as the coalescence behaviors of the bubbles,[21] decreasing the DFS and FS formation. The smaller size of the bubbles can be attributed to the higher surface tension, while the smaller number of bubbles can be due to the viscosity of the liquid, which hinders its mobility, resulting in less coalescence.[22] A closer look over the liquid surface, during plasma treatment shows interesting evidence of the salt crystal nucleation onto bubbles surface (Fig. 4).

It is clear, therefore, that bubbles play a fundamental role in the production of flower of salt, even when plasma is used as a precipitation inducer. A careful analysis of the total masses of the FS, DFS films and also of the sedimented precipitates (SED) was carried out for different bittern densities. For each 3 h interval, plasma was applied during the last 0.17 h. Then, the FS, DFS and SED films were collected, dried, and weighed (Fig. 5). It is observed that the salt produced in the form of flower of salt was higher than the sedimented ones up to bittern densities below 1.250 g/cm3. In saltwork, the production of flower of salt is always lower than that produced in the present work. This result corroborates our hypothesis that bubbles strongly influence

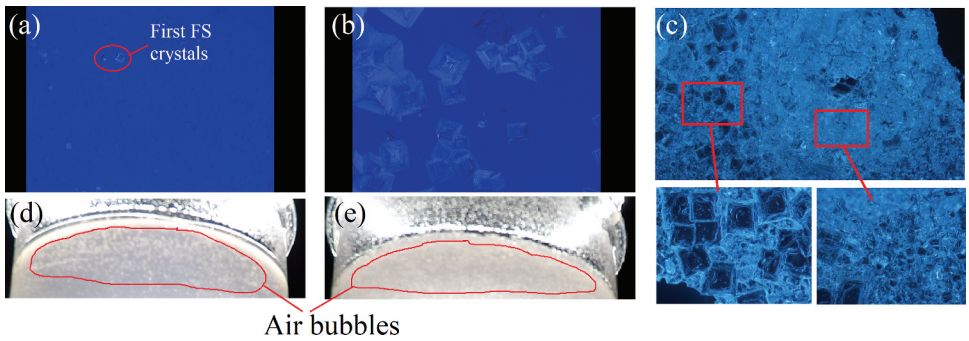

Figure 4. (A) Photograph obtained with the aid of a spectroscopic magnifying glass, 10 X amplification, of the DFS formed during plasma treatment in 1,238 g/cm3 saline solution. (B) Details, 135 X amplification, showing air bubbles as preferred sites for crystal nucleation.

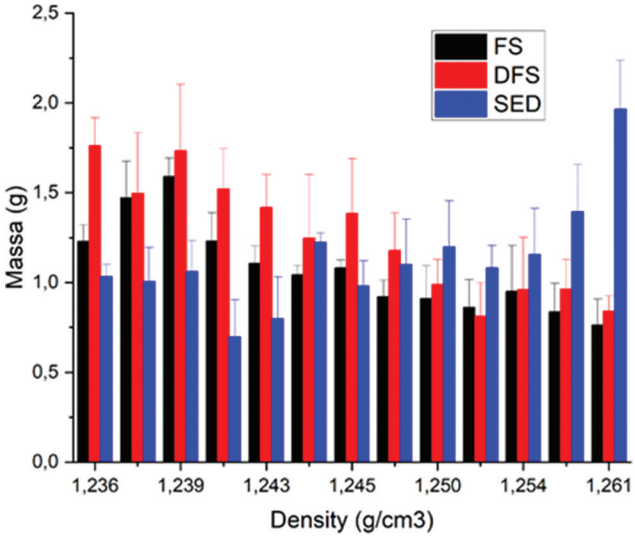

Figure 5. Total mass of FS, DFS and SED samples, extracted from bitterns with different densities.

the production of fleur de sel. For higher density values, the number, size, and mobility of the bubbles are reduced, justifying the reduction in the production of fleur de sel. It is also important to observe the DFS production efficiency, which was always superior to the FS, for all extractions. This value makes it more significant if we consider that the plasma activation time was only 0.17 h from the total evaporation time used for each interval.

The production of flower of salt in salt work is very rare, mainly due to the difficulty in controlling humidity and winds, thus justifying the high market price of this product.[17] Salt production in the salt industry is basically restricted to sedimented salts. In the case of laboratory production, humidity and winds can be controlled. Another difference from laboratory production is that the thermal flow happens from the bottom up, while in the saline this is not always the direction, which favors the formation of bubbles. Together these results provide important insights into mechanism of flower of salt formation. We insist, therefore, that this mechanism essentially depends on the existence of bubbles for the production of nucleating sites and for the buoyancy of the fleur de sel in the liquid. In addition, it was observed that the process is intensified when plasma is applied to the surface. These differences can be explained in part by the rapid localized heating produced of the PCD, which stimulates the formation of droplets[13,23–25] and also by the water dipole alignment caused by electric field that might be able to cause crystallization once the external electric field competes with the field of individual ions.[18,26]

Selective precipitation

Chemical analysis of FS, DFS and SED from solution during bittern evaporation, were performed. In addition to sodium, which is the major metallic element in the bittern, other important metals are potassium and magnesium. Observing the average value for three analyses, at each density, whose standard deviation was lower than 10%, concentration of these elements in relation to sodium, it is easier to compare selectivity in each sample (Fig. 6A). Likewise, since these elements are in the form of chlorides and/or sulfates, the comparison of these with sodium is also important (Fig. 6B). The most surprising result to emerge from the greater chemical selectivity in DFS. It is observed that the K/Na and Mg/Na ratios are higher in DFS samples, than in FS and SED samples, demonstrating that the plasma process was effective in selective extraction. The large variability of the concentration ratio found in the different bittern

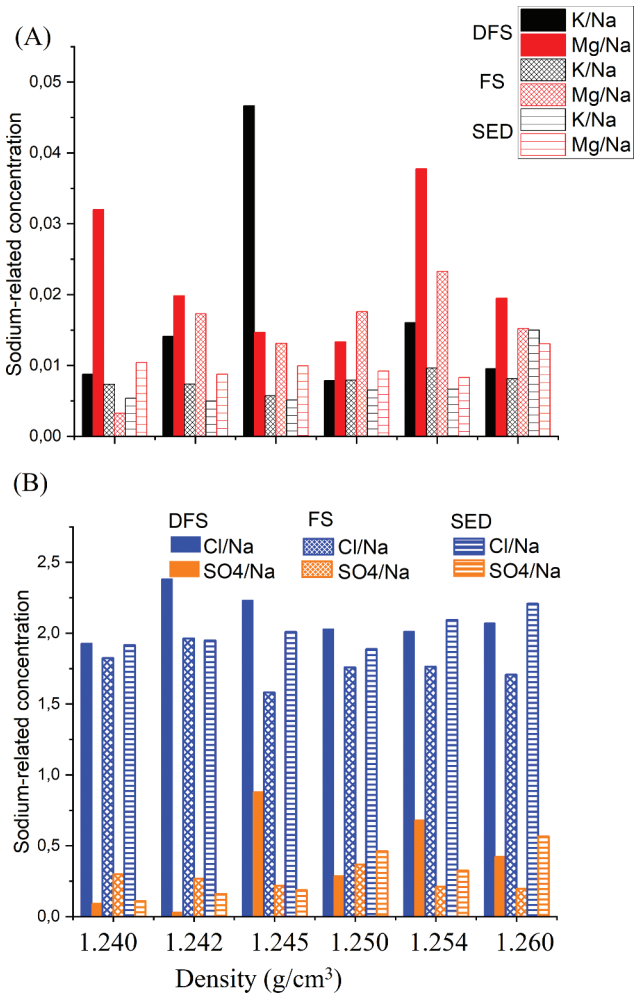

Figure 6. (A) Concentration of potassium and magnesium in relation to sodium for samples DFS, FS and SED; (B) Chlorine and sulfate concentration in relation to sodium for DFS, FS and SED samples.

densities (different evaporation times) are due to the precipitation dynamics for this density range. The only result in which the plasma was less selective for these two elements was for the solution with a density of 1.250 g/cm^3. In this case, it is observed that K/Na and Mg/Na were slightly smaller than FS and SED samples. In general, salts are formed by chlorides, mainly for solutions with lower densities. It is worth noting the SO4 values for the densities of 1.245 g/cm^3 and 1.254 g/cm^3, which presented the two highest relative concentration values for the DFS sample. These two solutions were the same that resulted in higher values for K and Mg, respectively, for the DFS sample.

Discussion

The present study was designed to determine the effect of PCD in the salt extraction from hypersaline water. However, due to the richness of the results simultaneous to those obtained during plasma treatment, it is necessary to discuss the different phenomena involved. Salt crystals were obtained in three different ways, namely: (i) by crystallization due to supersaturation of the bittern; (ii) by the formation of floating films called flower of salt (iii) the formation of floating films induced by plasma. The first case, thermodynamically predictable, occurs due to the increase in the concentration of solutes by evaporation of the solution, until reaching the limits of solubility of the salts, when then they are precipitated in the volume and then sedimented in the bottom of the container.[16] This is the natural process of producing sea salt by solar evaporation. In the second case there is the phenomenon of the production of fleur de sel that, despite being a commercially known product, its formation mechanism has been little known so far.[13] Its production takes place artisanal in salt flats, during solar evaporation. So far, little attention has been paid to understanding the mechanism of flower of salt formation, either in saltwork or laboratory. Some authors point out that the phenomenon occurs only on warmer days, with reduced humidity and wind speed.[27] Despite the importance of these variables, there is still a shortage of evidence on mechanism of the crystallization. We observed that during the evaporation of the liquid there was a convection movement of black dots (Fig. 7A) that we assume are air bubbles produced by heating the solution. We also found that the number of these bubbles was reduced as crystallization progressed (Fig. 7B), confirming research results in which the greater volume of air is entrained in salt than in freshwater to generate many more bubbles in salt water, but in very concentrated solutions the size and mobility of the bubbles are reduced.[20,28] We hypothesized that floating salts (FS and DFS) are produced following the same principle as flotation extraction, that is, only hydrophobic particles tend to attach with bubbles after collision.[22] Once that dissolved ions in solutions may alter the water structure, particle surface wettability and colloidal interactions between bubbles and particles,[22] we expect the extraction process to be strongly dependent on the concentration of solutes in the solution, that is, on its density. Based on the knowledge of the literature and our experimental observations, a model of nucleation and growth of grains of flower of salt was proposed. During the heating of the solution, air bubbles are released from water to the surface. Along the way they can collide with different

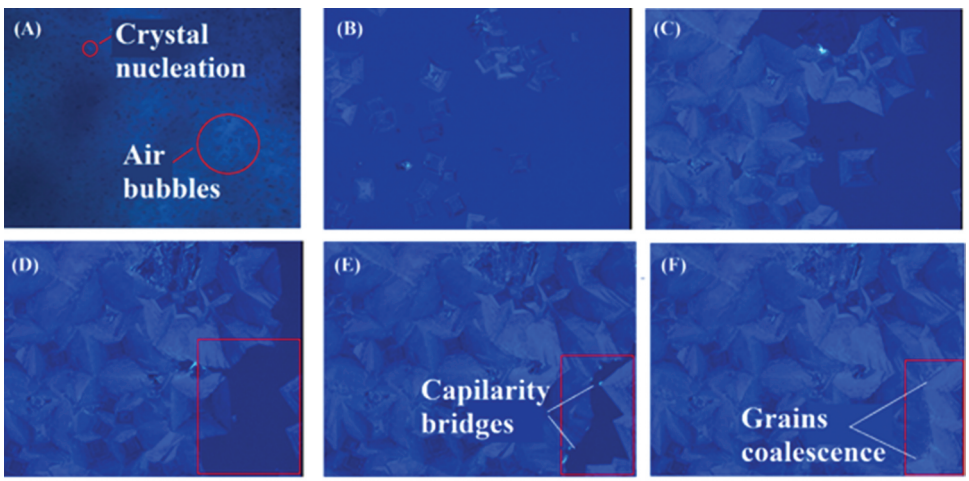

Figure 7. (A) Air bubbles (black dots) on surface of bittern during evaporation process and crystal nucleation; (B – C) Grain growth and film formation (D-F) Grains coalescence by the capillarity bridge, showing detail of the appearance of the capillarity bridge.

solvated ions, or even particles of salts, which will be attached if they are hydrophobic.[21,29] The compression of the electrical double layer in saline water enhances the thinning and rupture of the wetting film between bubbles and salt particles which are a critical step in the formation of a stable bubble-salt crystal, an important phenomenon in flower of salt production.[18] The coalescence of the crystals is done through capillarity bridges (Fig. 7C, D) produced under drying conditions, resulting in a crystal film. In the third case, formation of the DFS, the process is increased by the action of the plasma.

Studying the interaction of the plasma applied over a drop of hypersaline water, we observed that a cone-shaped deformation from the water surface to the cathode was formed. Crystal nucleation was observed inside the cone.[13] This effect has been demonstrated as an orientational reordering of the water molecules with their dipole moments parallel to the field, resulting in chains of aligned molecular dipole moments.[19] Another effect is the local heating of water, producing high evaporation. If the water conductivity is high enough and the pulse width is relatively long (usually from several microseconds to hundreds of microseconds), there will be a high-density current flow through the electrode tip because of the strong electric field strength.[24] Simultaneous to fast evaporation, droplets are produced inside solution increasing the nucleation rate of salt crystals.

Conclusions

The main goal of the current study was to assess the effect of plasma on mechanism and kinetics of flower of salt crystallization. Hypersaline solutions from effluents from the salt industry, called bittern, were treated by plasma, using pulsed corona discharge. From this treatment, three types of samples were collected, namely: (i) salt crystals (SED) produced by supersaturation, sedimented at the bottom of the container; (ii) Flower of salt (FS) crystals, floating films formed in regions without plasma action; (iii) Dense Flower of salt (DFS), formed under the action of plasma. The findings from this study make several contributions to the current literature. First, it contributes to our understanding of the mechanism of formation of the flower of salt, even under the action of plasma. It also shows that it is possible to extract salts, by dissolved air flotation, from hypersaline waters, at a rate higher than that of natural evaporation. It also shows that plasma can be used to enhance the extraction and selectivity of salts. These results add to the rapidly expanding field of desalination and wastewater treatment technology.

Acknowledgements

This project was funded by the National Council for Scientific and Technological Development (CNPQ- 430863/2016-0), the National Institute of Surface Engineering (CNPq- 465423/2014-0), and the National Council for the Improvement of Higher Education (CAPES).

Disclosure statement

No potential conflict of interest was reported by the author(s).

Funding

This work was supported by the CNPQ [430863/2016-0,430863/2016-0, 465423/2014-0];CAPES;

References

[1] Davies, P. A.; Knowles, P. R. Seawater Bitterns as a Source of Liquid Desiccant for Use in Solar-cooled Greenhouses. *Desalination*. 2006, 196, 266–279. DOI: 10.1016/j.desal.2006.03.010.

[2] Chung, T. S.; Zhang, S.; Wang, K. Y.; Su, J.; Ling, M. M. Forward Osmosis Processes: Yesterday, Today and Tomorrow. *Desalination*. 2012, 287, 78–81. DOI: 10.1016/j.desal.2010.12.019.

[3] Cath, T. Y.; Childress, A. E.; Elimelech, M. Forward Osmosis: Principles, Applications, and Recent Developments. *J. Memb. Sci.* 2006, 281, 70–87. DOI: 10.1016/j.memsci.2006.05.048.

[4] Darvishmanesh, S.; Pethica, B. A.; Sundaresan, S. Forward Osmosis Using Draw Solutions Manifesting Liquid-liquid Phase Separation. *Desalination*. 2017, 421, 23–31. DOI: 10.1016/j.desal.2017.05.036.

[5] Abdulbari, H. A.; Basheer, E. A. M. Microfluidics Chip for Directional Solvent Extraction Desalination of Seawater. *Sci. Rep.* 2019, 9, 1–11. DOI: 10.1038/s41598-019-49071-7.

[6] Stanisz, E.; Werner, J.; Zgoła-Grześkowiak, A. Liquid-phase Microextraction Techniques Based on Ionic Liquids for Preconcentration and Determination of Metals. *TrAC - Trends Anal. Chem.* 2014, 61, 54–66. DOI: 10.1016/j.trac.2014.06.008.

[7] Gabrić, B.; Sander, A.; Cvjetko Bubalo, M.; Macut, D. Extraction of S- and N-compounds from the Mixture of Hydrocarbons by Ionic Liquids as Selective Solvents. *Sci. World. J.* 2013, 2013, 512953,11. DOI: 10.1155/2013/512953.

[8] Hussein, A. A.; Zohdy, K.; Abdelkreem, M. Seawater Bittern a Precursor for Magnesium Chloride Separation: Discussion and Assessment of Case Studies. *Int. J. Waste Resour.* 2017, 07, 1–6. DOI: 10.4172/2252-5211.1000267.

[9] Al Mutaz, I. S.; Wagialia, K. M. Production of Magnesium from Desalination Brines. *Resour. Conserv. Recycl.* 1990, 3, 231–239. DOI: 10.1016/0921-3449(90)90020-5.

[10] Witzke, M.; Rumbach, P.; Go, D. B.; Sankaran, R. M. Evidence for the Electrolysis of Water by Atmospheric-pressure Plasmas Formed at the Surface of Aqueous Solutions (Journal of Physics D: Applied Physics (2012) 45 (442001)). *J. Phys. D Appl. Phys.* 2013, 46, 442001. DOI: 10.1088/0022-3727/46/12/129601.

[11] Rumbach, P.; Witzke, M.; Sankaran, R. M.; Go, D. B. Decoupling Interfacial Reactions between Plasmas and Liquids: Charge Transfer Vs Plasma Neutral Reactions. *J. Am. Chem. Soc.* 2013, 135, 16264–16267. DOI: 10.1021/ja407149y.

[12] de Barauna, J. B. F.; Pereira, O.; Gonçalves, I. A.; Vitoriano, J. O.; Alves-Junior, C. Sodium Chloride Crystallization by Electric Discharge in Brine. *Mater. Res.* 2017, 20, 215–220. DOI: 10.1590/1980-5373-MR-2017-0108.

[13] Almada, L. F. A.; Fontes, K. E. S.; Vitoriano, J. O.; Melo, V. R. M.; Fraga, F. E. N.; Alves-Junior, C. Applying Pulsed Corona Discharge in Hypersaline Droplets. *J. Phys. D Appl. Phys.* 2021, 54, 055202. DOI: 10.1088/1361-6463/abbb06.

[14] Rodrigues, C. M.; Bio, A.; Amat, F.; Vieira, N. Artisanal Salt Production in Aveiro/Portugal - an Ecofriendly Process. *Saline Syst.* 2011, 7, 1–14. DOI: 10.1186/1746-1448-7-3.

[15] Hawaidi, E. A. M.; Mujtaba, I. M. Simulation and Optimization of MSF Desalination Process for Fixed Freshwater Demand: Impact of Brine Heater Fouling. *Chem. Eng. J.* 2010, 165, 545–553. DOI: 10.1016/j.cej.2010.09.071.

[16] Sainz-López, N.; Boski, T.; Sampath, D. M. R. Fleur de Sel Composition and Production: Analysis and Numerical Simulation in an Artisanal Saltern. *J. Coast. Res.* 2019, 35, 1200–1214. DOI: 10.2112/JCOASTRES-D-18-00132.1.

[17] Donadio, C.; Bialecki, A.; Valla, A.; Dufossé, L. Carotenoid-derived Aroma Compounds Detected and Identified in Brines and Speciality Sea Salts (Fleur de Sel) Produced in Solar Salterns from Saint-Armel (France). *J. Food Compos. Anal.* 2011, 24, 801–810. DOI: 10.1016/j.jfca.2011.03.005.

[18] Vanraes, P.; Bogaerts, A. Plasma Physics of Liquids — A Focused Review. *Appl. Phys. Rev.* 2018, 5, 1–56. DOI: 10.1063/1.5020511.

[19] Gungoren, C. An Investigation of Air/water Interface in Mixed Aqueous Solutions of KCl, NaCl, and DAH. *Physicochem. Probl. Miner. Process.* 2019, 5, 1259–1270. DOI: 10.5277/ppmp19050.

[20] Wu, J. Bubbles Produced by Breaking Waves in Fresh and Salt Waters. *J. Phys. Ocean.* 2000, 30, 1809–1813. DOI: 10.1175/1520-0485(2000)030<1809:BPBBWI>2.0.CO;2.

[21] Wang, B.; Peng, Y. The Effect of Saline Water on Mineral Flotation - A Critical Review. *Miner. Eng.* 2014, 66, 13–24. DOI: 10.1016/j.mineng.2014.04.017.

[22] Shokri-Kuehni, S. M. S.; Norouzi Rad, M.; Webb, C.; Shokri, N. Impact of Type of Salt and Ambient Conditions on Saline Water Evaporation from Porous Media. *Adv. Water Resour.* 2017, 105, 154–161. DOI: 10.1016/j.advwatres.2017.05.004.

[23] Shirai, N.; Ichinose, K.; Uchida, S.; Tochikubo, F. Influence of Liquid Temperature on the Characteristics of an Atmospheric Dc Glow Discharge Using a Liquid Electrode with a Miniature Helium Flow. *Plasma Sources Sci. Technol.* 2011, 20, 034013. DOI: 10.1088/0963-0252/20/3/034013.

[24] Dubinov, A. E.; Lyubimtseva, V. A. Crystallization Features of Aqueous Solutions in Their Droplets Evaporated by Nanosecond Spark Discharge Treatment. *High Energy Chem.* 2019, 53, 3–6. DOI: 10.1134/S001814391901003X.

[25] Kruszelnicki, J.; Lietz, A. M.; Kushner, M. J. Atmospheric Pressure Plasma Activation of Water Droplets. *J. Phys. D Appl. Phys.* 2019, 52, 355207. DOI: 10.1088/1361-6463/ab25dc.

[26] Jirsak, J.; Mouc, F.; Nezbeda, I. Insight into Electrospinning via Molecular Simulations. *Ind. Eng. Chem. Res.* 2014, 53, 8257–8264. DOI: 10.1021/ie404268f.

[27] VIEIRA AS. Caracterização da cinética de formação da Flor de Sal (Issue Universidade de Aveiro) [University of Aveiro]., 2015. http://hdl.handle.net/10773/15480

[28] Slauenwhite, D. E.; Johnson, B. D. Bubble Shattering: Differences in Bubble Formation in Fresh Water and Seawater. *J. Geophys. Res. Ocean.* 1999, 104, 3265–3275. DOI: 10.1029/1998jc900064.

[29] Wu, Z.; Wang, X.; Liu, H.; Zhang, H.; Miller, J. D. Some Physicochemical Aspects of Water-soluble Mineral Flotation. *Adv. Colloid Interface Sci.* 2016, 235, 190–200. DOI: 10.1016/j.cis.2016.06.005.